CrossMark

Determination of activation energy as a function of conversion for the oxidation of heavy and light crude oils in relation to in situ combustion

Milad Karimian[1,2] · Mahin Schaffie[1] · Mohammad Hassan Fazaelipoor[3]

Abstract Efficient design of in situ combustion depends on accurate kinetic study of crude oil oxidation. We aimed to study the variation of activation energy in both heavy and light crude oils. TG/DTG and DSC performed under atmospheric air from 100 to 800 °C in four different heating rates. Three distinct reaction regions were observed known as low-temperature oxidation, fuel deposition and high-temperature oxidation. Increase in heating rate shifted onset of oxidation reactions to higher temperatures. Three isoconversional kinetic models were also used to analyze the conversion dependence of the activation energy (E_α). Reaction regions were analyzed separately because their reactions schemes are not the same. The estimated E_α values of different models at each degree of conversion were nearly similar. Activation energy of crude oil varied considerably with conversion in some reaction regions. Therefore, average value of activation energy is not always a reliable parameter for in situ combustion models.

Keywords Crude oil · Oxidation reaction · Activation energy · Thermal analysis · Isoconversional kinetic models

✉ Milad Karimian
milad.karimian@gmail.com

[1] Department of Petroleum Engineering, Shahid Bahonar University of Kerman, Kerman, Iran

[2] Society of Young Researchers, Shahid Bahonar University of Kerman, Kerman, Iran

[3] Department of Chemical Engineering, Shahid Bahonar University of Kerman, Kerman, Iran

Introduction

Modern economies are tightly bounded to energy and fossil fuels are, still, the most important sources of energy. Heavy oil resources estimated to exceed conventional oil resources [1, 2]. The urge to use these unconventional reservoirs raised the need for improving thermal methods of enhanced oil recovery (EOR) such as in situ combustion (ISC). Heterogeneous chemical reactions complicated ISC modeling. Predictability and success of an ISC project directly depend on the clear understanding of the process and reaction kinetic.

Thermogravimetric (TG) analysis and differential scanning calorimetry (DSC) are common methods to study chemical reaction kinetics. The first implementation of thermal analysis for crude oils dates back to 1959 which Tadema [3] used differential thermal analysis (DTA) to study crude combustion and determined two exothermic reaction regions. Since then, many investigators have studied combustion kinetics using TG/DTG and DSC methods [4–8]. Drici and Vossoughi [9] investigated the effect of surface area on oxidation via TG/DSC, and using single heating rate analysis, the activation energy was calculated. Kok et al. [10–13] characterized combustion properties of fossil fuels using TG/DTG, DTA and DSC methods under different pressures. The combustion process was divided into three reaction regions known as low-temperature oxidation (LTO), fuel deposition (FD) and high-temperature oxidation (HTO). Some investigators [13, 14] considered FD as a sub region of LTO reactions; therefore, in LTO reaction regions, in addition to distillation of volatile hydrocarbons and oxidation of the light hydrocarbons, coke is formed and deposited on the solid matrix as fuel for in situ combustion process.

According to studies of oxidation behavior of crude oil fractions based on single heating rate TG analysis [15–18], it was suggested that asphaltene affect coke formation more than other components. Kok and Gul [14, 19] studied oxidation behavior of crude oil and its saturated, aromatic and resin fractions using multiple heating rates TG and DSC analysis. They observed that resins lose considerable mass in HTO region, while saturates, lose most mass in LTO region and saturates gave minimum heat of reaction. Nonetheless, Freitag and Verkoczy [20] showed that models which separately study saturated, aromatic, resin and asphaltene (SARA) fractions are not accurate and realistic. They suggested studying the effect of saturate components in the presence of other SARA fractions; otherwise, LTO kinetic results deviate from reality.

Brief review of the literatures reveals that most of studies about thermal analysis of crude oils focus on quantitative kinetic modeling. Consequently, various kinetic models are used. Some investigators [21–25] assumed a generalized reaction scheme and tried to find the stoichiometric coefficients of each reaction. These methods are faced with a systematic error due to neglected or

simplified reactions. Another popular approach is model fitting [11, 26–29] which assumes a reaction model and resolves kinetic triplet. This method also suffers from the same error as generalized reaction scheme. Isoconversional kinetic models use multiple heating programs to evaluate E_α and bypass estimation of reaction models [30–34].

In this paper, TG/DTG and DSC methods were used to study the combustion behavior of heavy and light crude oils. According to International Confederation of Thermal Analysis and Calorimetry (ICTAC) recommendations, the test was performed with four different non-isothermal heating programs. We evaluated E_α using three isoconversional methods and investigated the conversion dependence for main oxidation reaction regions.

Materials and methods

Samples of crude oils were provided from two oil reservoirs, located southwest of Iran. The composition of both samples is compared in Fig. 1. Reservoir and crude oil characteristics are given in Table 1. Crude oil density was
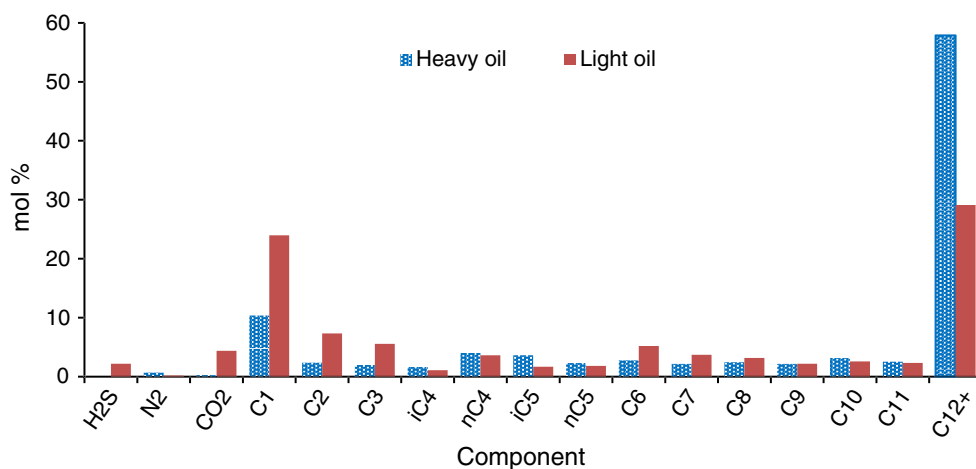
Fig. 1 Composition of crude oil samples

Table 1 Reservoir and sample characteristics

Property	Heavy oil	Light oil
Reservoir depth from sea level/m	1100 (top), 1200 (bottom)	3350 (top), 3750 (bottom)
Maximum reservoir pressure, $P_{R,max}$/kPa	10,853	35,853
Bubble point pressure, P_b/kPa	6308	9846
Reservoir temperature, T_R/°C	59	110
Oil specific gravity, *sp. gr.*	0.9806	0.9081
Oil density, ρ_o/°API	12.8	24.3
Water density, ρ_w/g cm^{-3}	1	1
Oil viscosity at saturation pressure, μ_{ob}/cP	1654 at 59 °C	1.56 at 110 °C
Oil formation volume factor, B_o/bbl STB^{-1}	1.05 at 6308 kPa	1.18 at 9846 kPa
	1.03 at 10,583 kPa	1.33 at 13,431 kPa

Table 2 SARA fractions of crude oils (values in mass percent)

Sample name	Saturates	Aromatics	Resins	Asphaltene
Heavy oil	12.3	21.7	51.3	14.7
Light oil	52.8	30.5	5.7	11.0

determined in accordance with ASTM D4052; a small volume (approximately 0.7 mL) of liquid sample is introduced into an oscillating sample tube, and the change in oscillating frequency caused by the change in the mass of the tube determines the density of the sample. SARA fractions obtained according to ASTM D-2007 which is based on the selective adsorption of polar and aromatic compounds on clay and silica gel, respectively. Saturated hydrocarbons have low affinity for both clay and silica; therefore, saturates can be eluted by n-pentane. Polar and aromatic compounds are recovered from clay and silica gel using appropriate solvents. The separated components are determined after solvent evaporation. SARA fractions are given in Table 2.

Thermogravimetry (TG) and differential scanning calorimetery (DSC) analyses were performed by *NETZSCH 409 PG Luxx* simultaneous thermal analysis (STA) system. STA measures sample mass with 0.001 mg precision. Oxidation of crude oil causes self-heating; this effect would induce temperature gradients within sample which results in unreliable temperature readings [35]. To avoid such errors, the sample thickness decreased to 100 μm and high conductivity crucibles (platinum) were used.

Prior to experiments, the instrument must be calibrated for temperature readings [36, 37]; since platinum crucibles form alloy with metals, five organic and inorganic reference materials were used. Transition temperatures of these substances cover ranges from room temperature to 900 °C. Standard error of calibration was ±1.0 °C. Two calibration tests (with $RbNO_3$ and Ag_2SO_4) were repeated before measurements; standard error of reproducibility experiments was ±0.3 °C. Buoyancy calibration was also performed for each heating rate before TG measurements.

Samples first heated up to 100 °C, at heating rate (β) of 15 °C min^{-1} in N_2 atmosphere to reach the original reservoir temperature without prior oxidation. A short (5 min) isothermal step stabilized temperature before oxidation step. Finally samples heated up to 800 °C in an oxidizing atmosphere, consisting 50 mL min^{-2} air and 10 mL min^{-2} N_2 protective gas. Some experiments were replicated to check repeatability of TG/DSC measurements; results of paired samples t test showed that the correlation is significant at the 0.01 level (i.e., 99 % confidence in similarity of replications).

According to ICTAC recommendations [38], a reliable kinetic experiment should consist three to five different heating rates, all <20 °C min^{-1}; so, we heated samples with four different linear heating rates (5, 9, 14 and 18 °C min^{-1}). There might be a significant systematic variation in the mass loss curves for samples of different masses [38]; therefore, it was tried to use samples with fixed size (± 0.1 mg) for each crude oil at different heating rates.

Results and discussion

DSC test results

Figure 2 shows DSC curves of light oil sample for all heating rates. Kok and Topa [8] mentioned that increasing heating rate increases the pick amplitude and its corresponding temperature. This is evident in Fig. 2 which reaction zones shifted right as the heating rate increased; peaks are also amplified whereas their domain decreased. More heat is released in less time and total heat flow is relatively constant under similar peaks at different heating rates. This is in accordance with the isoconversional principle which states: "process rate at constant extent of conversion is only a function of temperature" [35].

Some investigators [5, 39] proposed that after a distillation period, three major stages exist known as low-temperature oxidation (LTO), fuel deposition (FD) and high-temperature oxidation (HTO) regions. Crude oil consists of numerous fractions in different quantities (Fig. 1); therefore, various reactions take place during the course of combustion. Despite such variation, it has been shown that different crude oils exhibit similar reaction zones when heated in air atmosphere [40]. Hence, comparing different crude oils according to their thermal behavior would be valid.

Figure 3 compares the DSC results of heavy and light oils. It is evident that reactions in heavy oil sample commenced at relatively higher temperatures and HTO peak is larger than that of the light crude sample. For example, at a heating rate of 9 °C min^{-1}, HTO peak of heavy oil appeared at 540 °C and its amplitude was 7.776 mW mg^{-1}. Temperature of HTO peak in light oil was relatively the same as the heavy crude sample (539 °C), but peak height was 4.688 mW mg^{-1}. The area under the peaks demonstrates the released heat, which is 1680 and 8022 J g^{-1} for light and heavy crude samples, respectively. It was suggested [18] that the content of the colloidal composition (i.e., asphaltene and resin) has a remarkable influence on the fuel formation, its properties and therefore fuel combustion (i.e., HTO). Figure 1 and Table 2 show that the percentage of heavier fractions in heavy oil is far more than that of the light oil. Thus, in addition to increased concentration of fuel, more reactive fuel is also available for combustion of heavier oils [18] which justify release of more heat during HTO. It is also

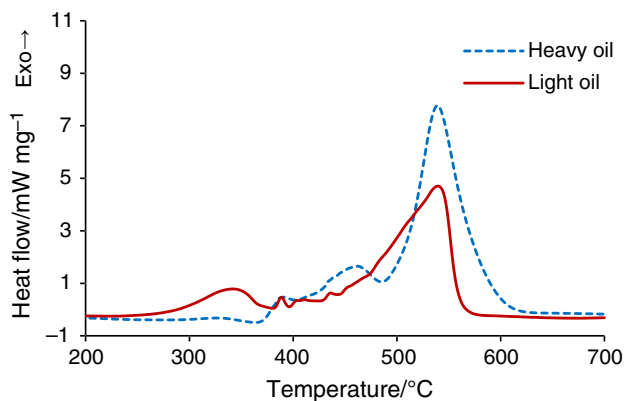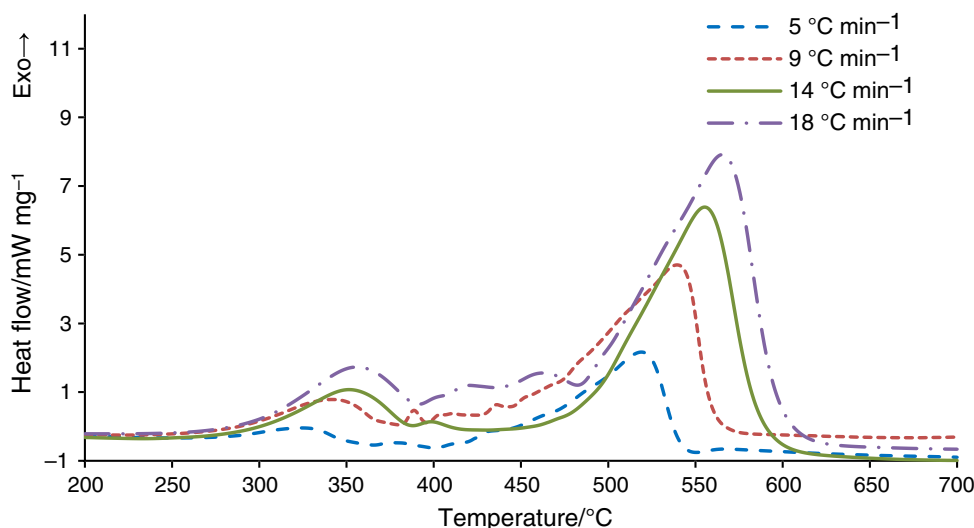**Fig. 2** DSC curve of light oil combustion in different heating rates

Fig. 3 Comparison of DSC curves for heavy and light oil at a heating rate of 9 °C min^{-1}

observed that LTO peak in light oil is much bigger than heavy oil peak (272 and 68.59 J g^{-1} for light and heavy oil samples, respectively). Lighter components of oil mostly contribute in LTO reactions [41]. These components are converted to heavier oxygenated products such as alcohols, aldehydes, ketones, hydroperoxides and carboxylic acids [22]. Later, these LTO products participate in FD and HTO reactions [42]. According to Fig. 1 and Table 2, the light oil contains more light fractions than heavy oil; therefore, more heat is released during LTO reactions of the light oil sample.

TG/DTG results

Figure 4 compares TG and DTG results of the light oil sample in different heating rates. Once again, similar trends of mass loss and DTG are observed for all heating rates. Reaction regions can be identified from DTG curve whose ranges are similar to estimated regions from DSC. As mentioned earlier, increasing heating rate shifts the

onset of reactions to higher temperature, which cause TG curves to decline later, in higher temperatures. At higher heating rates, amplitude of DTG curve is increased because reaction rate (and therefore mass loss) is increased.

It must be noted that differentiating experimental data of the integral nature (i.e., TG data) has a drawback because derivation is sensitive to the noise of experimental data [35] and estimation of dα/dt amplifies that noise. Therefore, smoothing data prior to differentiation is necessary. Integral methods of kinetic analysis can bypass the differentiation, so they are proper for TG data modeling. Differential methods (e.g., Friedman) would deal better with differential data like DSC.

Reaction intervals, mass loss and peak temperature (T_{peak}) of reaction regions are presented in Table 3. T_{peak} is a temperature at which maximum rate of reaction occurs. It is obtained from TG/DTG and DSC curves.

In LTO region, vaporization of free water and light hydrocarbons is the major reason of mass loss; therefore, light oil is susceptible to more mass loss [34]; this is evident in Table 3, oxygen is consumed during LTO to form partially oxygenated hydrocarbons which are more dense and viscous. It is believed that these oxygenated compounds, later, play an important role in formation of fuel [29, 41]. Mechanism of LTO is complicated because it consists of multiple concurrent reactions. Varfolomeev et al. [34] proposed that the asphaltene content increased considerably after LTO while resin content decreased. Ranjbar and Pusch [18] suggested that asphaltenes are primary transient products of the conversion of resins into coke. The heavy oil lost more mass in both FD and HTO regions compared to the light oil. It might be due to higher amounts of asphaltene components in heavy oil. Asphaltene molecules are resistant to heat and exhibit very low mass loss in distillation and LTO regions.

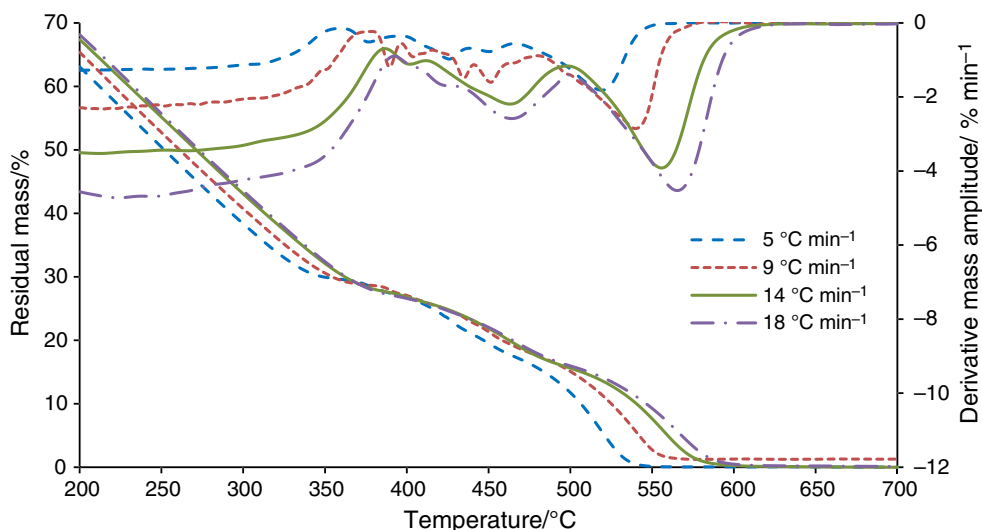**Fig. 4** TG/DTG curves of the light oil sample at different heating rates

Table 3 Reaction intervals, mass loss and peak temperature of light and heavy oil

Crude oil, heating rate/ °C min⁻¹	LTO			FD			HTO		
	Reaction interval/°C	Mass loss/%	Peak temp./°C	Reaction interval/°C	Mass loss/%	Peak temp./°C	Reaction interval/°C	Mass loss/%	Peak temp./°C
Light oil									
5	110–358	54.1	324	358–466	12.2	426	466–542	17.0	519
9	110–378	55.0	342	378–480	11.1	435	480–560	16.0	539
14	110–387	55.4	351	387–497	11.9	463	497–588	15.3	555
18	110–392	55.9	356	392–500	11.1	464	500–599	15.5	565
Heavy oil									
5	110–398	45.3	375	398–476	19.7	428	476–537	26.8	515
9	110–413	44.9	388	413–497	22.6	454	497–581	25.6	540
14	110–409	45.2	397	409–506	20.8	462	506–604	25.4	562
18	110–416	45.4	402	416–513	21.7	470	513–635	25.8	573

Low-temperature oxidation region was the broadest temperature interval ($\Delta T_{\mathrm{light}} = 269 \pm 7\ °C$ for light oil and $\Delta T_{\mathrm{heavy}} = 299 \pm 4\ °C$ for heavy oil). FD region of light oil was to some extent wider than that of the heavy oil ($\Delta T_{\mathrm{light}} = 107 \pm 2\ °C$ vs. $\Delta T_{\mathrm{heavy}} = 98 \pm 4\ °C$). Contrary, HTO region of heavy oil was slightly wider ($\Delta T_{\mathrm{light}} = 87 \pm 4\ °C$ and $\Delta T_{\mathrm{heavy}} = 91 \pm 11\ °C$).

According to Fig. 5, light crude oil showed a relatively high total mass loss ($\approx 70\ \%$) before FD region, whereas less mass loss was associated with HTO (16 %) and FD regions (11 %) in a smaller temperature window. The hump in DTG and DSC curves of light oil suggests the joint effect of distillation and LTO is responsible for such huge reduction in remaining mass from 110 °C to about 378 °C. In contrast, less mass decreased in heavy oil sample during LTO (45 %), while mass loss in FD and HTO increased (23 and 26 %, respectively). As discussed before, higher extent of fuel forming fractions in heavy oil

enhanced FD reactions and consequently more fuel is deposited for HTO. On the other hand, less distillation and LTO reaction are a sign of lower extent of light fractions of oil which is confirmed by Fig. 1 and Table 2.

It is worth noting that about 5 % of heavy oil and 15 % of light oil samples were evaporated within 0–100 °C region (first 5 min of the test) in the pure N_2 atmosphere.
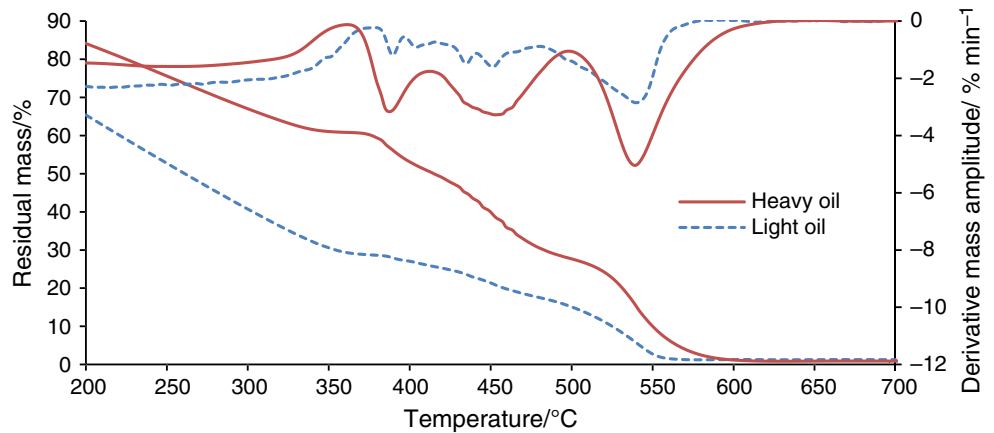
Kinetic modeling

The rate of combustion reactions can be parameterized in terms of T and α as:

$$\frac{\mathrm{d}\alpha}{\mathrm{d}t} = k(T)f(\alpha) = A \exp\left(\frac{-E}{RT}\right)f(\alpha) \tag{1}$$

where T is temperature, t is time, α is the extent of conversion, $f(\alpha)$ is the reaction model and $k(T)$ is the rate constant which is represented by Arrhenius equation. In

that equation, A is the preexponential factor, E is the activation energy and R is the gas constant. Equation (2) can be used to obtain α from experimental results.

$$\alpha = \frac{m_i - m}{m_i - m_f} \quad (2)$$

where m is the percentage of the residual mass of the sample at time t. m_i and m_f are the initial and the final mass of the sample. As stated in the previous section, it is best to interpret TG data with integral methods rather than differential methods (Eq. 1). Integration of Eq. (1) for isothermal conditions yields:

$$g(\alpha) = \int_0^\alpha \frac{d\alpha}{f(\alpha)} = A \exp\left(\frac{-E}{RT}\right) t \quad (3)$$

where $g(\alpha)$ is the integral form of the reaction model. Solving above equation requires an assumption of reaction model. In complex heterogeneous reaction (e.g., crude oil combustion), many models largely simplify the real reaction model and do not show significantly different results,

especially in certain ranges of α [35]; fitting such models to experimental data would be erroneous. Alternatively, it is possible to bypass such assumption by using multiple heating rates. Isoconversional principle states that the process rate at constant extent of conversion is only a function of temperature [35]. Non-isothermal experiments mostly use constant heating rate (β) which means $T = T_0 + \beta \times t$ or $dT/dt = \beta$. Therefore, rearranging Eq. (1) and integrating give below equation:

$$g(\alpha) = \frac{AE}{\beta R} \int_x^\infty \frac{\exp(-x)}{x^2} dx = \frac{AE}{\beta R} p(x) \quad (4)$$

Equation (4), $p(x)$ has no analytical solution, and different approximation methods are proposed to solve it. Ozawa, Flynn and Wall (OFW) Method [43, 44] is based on Doyle approximation of $p(x)$ [45]; Therefore, Eq. (4) can be rearranged to obtain Eq. (5):

$$\ln(\beta_i)_\alpha = \ln\left(\frac{AE_\alpha}{g(\alpha)R}\right) - 5.330 - \frac{1.052 E_\alpha}{RT_{\alpha,i}} = \quad (5)$$
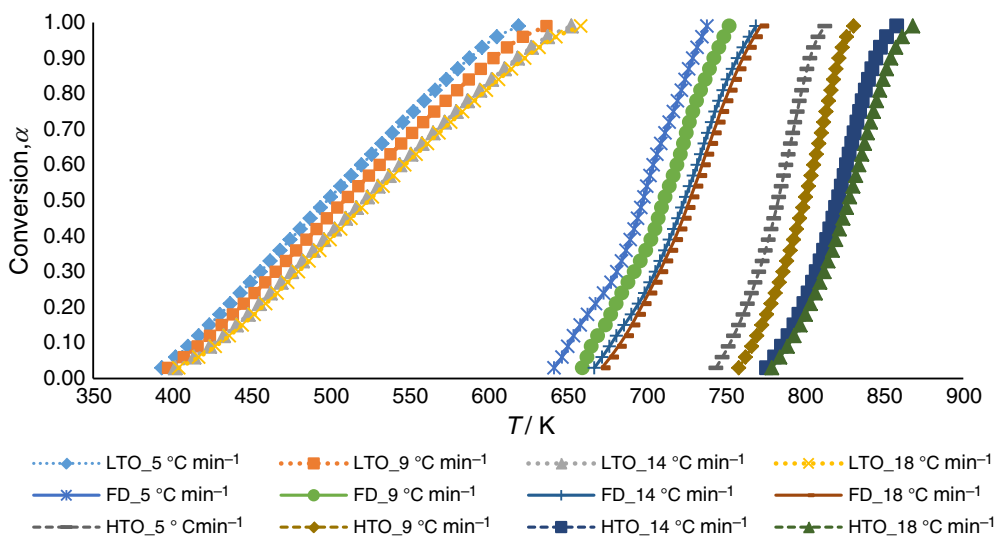

Fig. 6 Variation of conversion degree with temperature at different heating rates and different reaction regions

Fig. 7 OFW kinetic curve for FD region of heavy oil at different extents of conversion
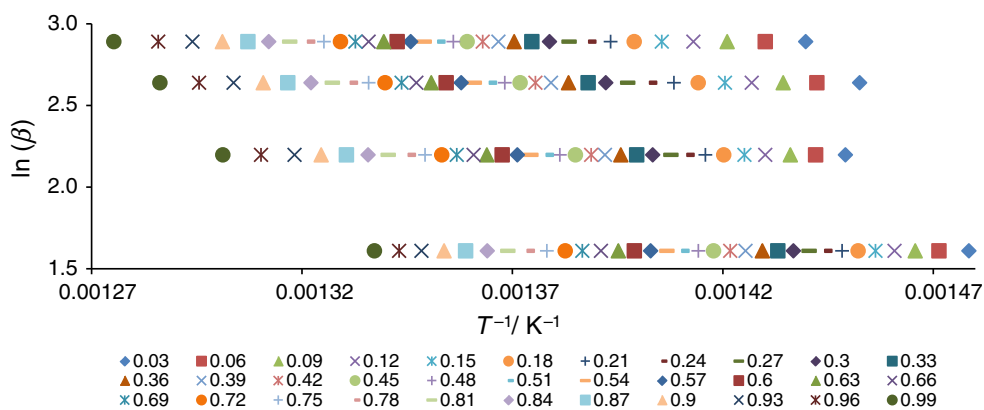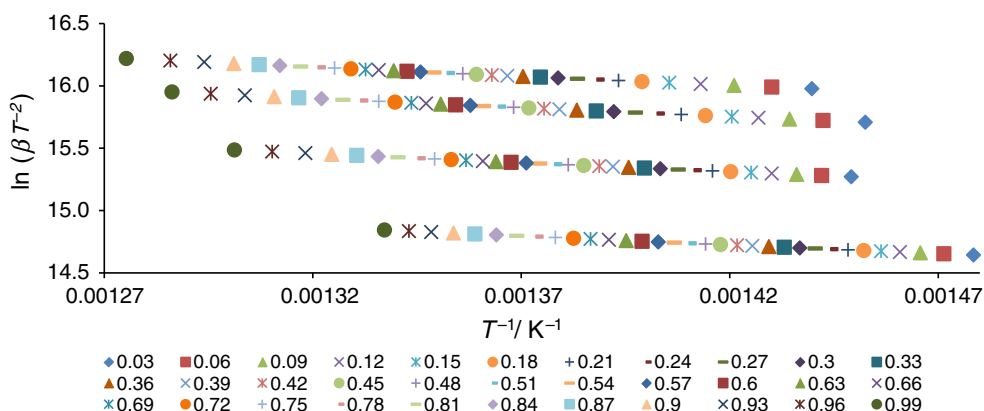

◆0.03	■0.06	▲0.09	×0.12	✳0.15	●0.18	+0.21	−0.24	—0.27	◆0.3	■0.33
▲0.36	×0.39	✳0.42	●0.45	+0.48	−0.51	—0.54	◆0.57	■0.6	▲0.63	×0.66
✳0.69	●0.72	+0.75	−0.78	—0.81	◆0.84	■0.87	▲0.9	×0.93	✳0.96	●0.99

Fig. 8 KAS kinetic curve for FD region of heavy oil at different extents of conversion

|										
◆0.03	■0.06	▲0.09	×0.12	✳0.15	●0.18	+0.21	−0.24	—0.27	◆0.3	■0.33
▲0.36	×0.39	✳0.42	●0.45	+0.48	−0.51	—0.54	◆0.57	■0.6	▲0.63	×0.66
✳0.69	●0.72	+0.75	−0.78	—0.81	◆0.84	■0.87	▲0.9	×0.93	✳0.96	●0.99

where i indicates heating rates. E_α is estimated from slope of the linear plot of $\ln(\beta_i)$ against $1/T_{\alpha,i}$. Finding the slope for different αs reveals the dependency of E_α on α.

Kissinger, Akahira and Sunose (KAS) also used a more precise approximation and obtained Eq. (6):

$$\ln\left(\frac{\beta_i}{T_{\alpha,i}^2}\right) = Const - \frac{E_\alpha}{R}\left(\frac{1}{T_{\alpha,i}}\right) \qquad (6)$$

Plot of $\ln(\beta\, T^{-2})$ versus T^{-1} for each α gives a straight line with slope of $-E_\alpha/R$. Starink [46] proposed even more

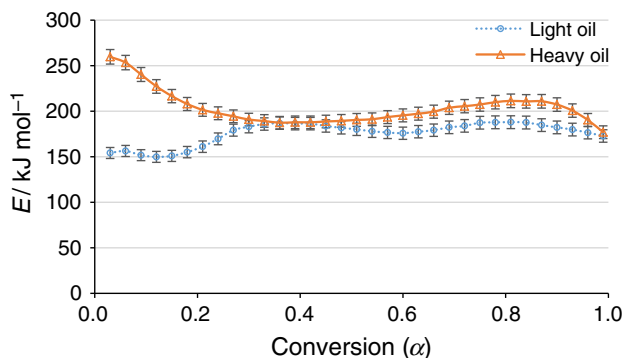**Fig. 9** Variation of activation energy of LTO reactions with conversion in heavy and light oil
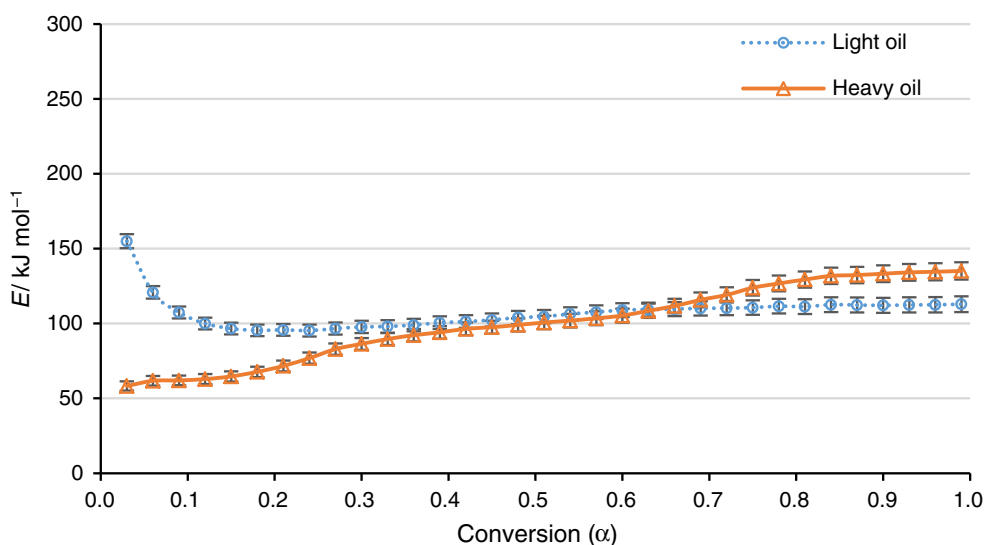
Fig. 10 Variation of activation energy of FD reactions with conversion in heavy and light oil

accurate approximation of $p(x)$. More accurate E_α can be obtained through Eq. (7):

$$\ln\left(\frac{\beta_i}{T_{\alpha,i}^{1.92}}\right) = Const - 1.0008\left(\frac{E_\alpha}{RT_{\alpha,i}}\right) \tag{7}$$

Fig. 11 Variation of activation energy of HTO reactions with conversion in heavy and light oil
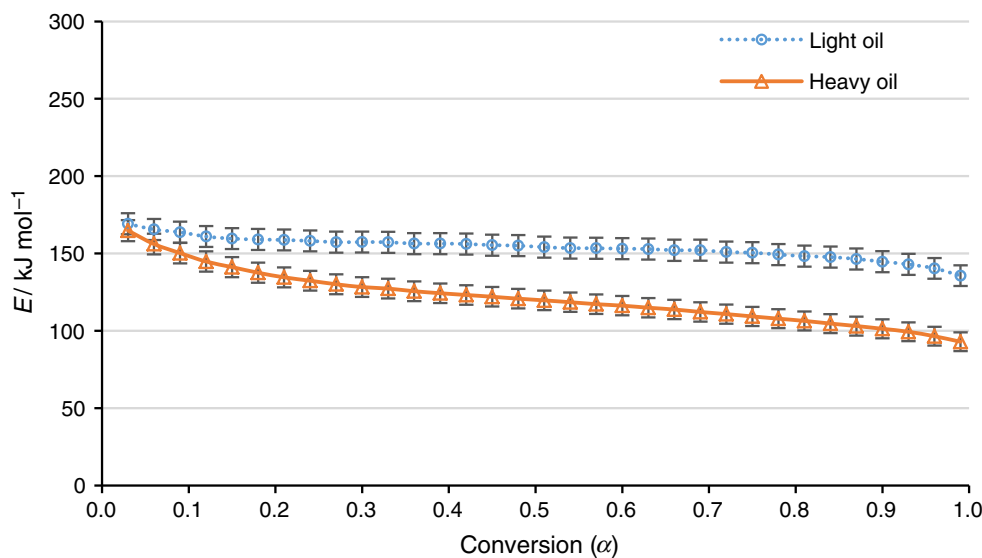
Before implementation of isoconversional methods, TG was divided into three reaction regions (LTO, FD and HTO) and TG signal of each region was separately normalized within 0–1 interval using Eq. (2) to obtain conversion degree (α) vs. temperature (T). Typically TG records so many data points. It is recommended [47] to perform kinetic analysis with a step ($\Delta\alpha$) of <0.05. It is unlikely that the experimental α versus T contain points exactly at selected values of α; therefore, one has to use interpolation or curve fitting to find T_α. This procedure was repeated for all reaction regions and all temperature programs (i.e., β values in case of linear program). Figure 6 illustrates variation of the conversion degree of light oil with temperature at different heating rates and different reaction regions with $\Delta\alpha = 0.03$.

After rearranging α–T data, OFW, KAS and Starink characteristic curves were plotted according to Eqs. (5)–(7) with $\Delta\alpha = 0.03$ for LTO, FD and HTO regions. For example, Figs. 7 and 8 show OFW and KAS characteristic curves for FD region of heavy oil, respectively. At each

Table 4 Average E_α/kJ mol^{-1} of crude oils by OFW, KAS and Starink methods

Kinetic models	Light oil			Heavy oil		
	LTO	FD	HTO	LTO	FD	HTO
OFW $\bar{E}_\alpha$ ($n = 33$)	98.31	98.31	140.18	91.44	189.29	108.85
KAS $\bar{E}_\alpha$ ($n = 33$)	111.98	111.98	160.83	104.99	211.16	128.05
Starink $\bar{E}_\alpha$ ($n = 33$)	111.64	111.64	160.29	104.64	210.68	127.50
Mean ($n = 3 \times 33$)	107	176	154	100	204	121
Standard deviation	10.68	12.14	6.89	24.70	18.32	16.91
Standard error of mean	6.17	7.01	3.98	14.26	10.58	9.76

extent of conversion, slope of the fitted line for all heating rates was found and apparent activation energies calculated by Eqs. (5)–(7).

The activation energy was obtained by OFW, KAS and Starink methods at each conversion degree. KAS and Starink methods estimated nearly the same E_α values, and results of OFW method were less than both. At each extent of conversion, average values of E_α from three isoconversional methods were calculated and plotted against conversion (α). Variation of activation energy of heavy and light oil was compared during LTO, FD and HTO regions in Figs. 9–11, respectively. Error bars indicate standard error of the averaging E_α of three methods at each conversion degree.

During LTO, apparent activation energy of light oil initially ($\alpha < 0.1$) decreased from 155 kJ mol^{-1} and remained relatively constant over rest of the LTO region. Mean activation energy of light oil ($n = 99$) was 107 ± 10.68 kJ mol^{-1} (Fig. 9). Firstly, activation energy of heavy oil was less than that of light oil (58 kJ mol^{-1}). However, E_α increased gradually (to 135 kJ mol^{-1}) and exceeded the E_α of the light oil. Average activation energy of heavy oil was 100 kJ mol^{-1} (standard deviation, SD = 24.70 kJ mol^{-1}).

In FD region, activation energy of light oil, first, increased from 150 kJ mol^{-1} to about 185 kJ mol^{-1} and then slightly fluctuated (SD = 4.5 kJ mol^{-1}) around 180 kJ mol^{-1} while activation energy of heavy oil first, decreased (from 260 to 185 kJ mol^{-1}) and then reached 198 ± 9.5 kJ mol^{-1}. Average E_α was 176 ± 12 and 204 ± 18 kJ mol^{-1} for heavy and light oils, respectively.

HTO reactions showed the reverse behavior compared to FD; activation energy of light oil was more than E_α of heavy oil in all conversions and E_α of light oil remained nearly constant ($\bar{E}_\alpha = 154 \pm 6.9$ kJ mol^{-1}). But E_α of heavy oil decreased continuously from 165 to 93 kJ mol^{-1}. During HTO, average activation energy of heavy oil was 100 ± 24.7 kJ mol^{-1}.

Average activation energy, SD and standard error of calculations for oil samples, reaction region and different kinetic models are summarized in Table 4.

Conclusions

Efficient design of in situ combustion process depends on the accurate kinetic modeling of oxidation reactions of crude oil. Thermal characterization and kinetics of oxidation reactions for heavy and light crude oil samples were investigated by simultaneous TG/DTG and DSC techniques. Data were modeled using three integral isoconversional kinetic models. Following concluding remarks can be presented.

- Increase in heating rate shifts onset of oxidation reactions to higher temperatures and caused more mass loss and heat flow. It also makes narrower peaks in DSC and DTG which means that as heating rate increases, the reactions proceed faster.
- According to TG/DTG and DSC results, three distinct reaction regions were observed during oxidation. These regions were also reported by several investigators [48–51].
- Low-temperature oxidation region was the broadest temperature interval, whereas HTO region was the narrowest one. Light crude oil was more susceptible to LTO reactions and heavy oils lost most of their residual mass during FD and HTO. In contrast to heavy oil, the light oil sample lost more mass during LTO and FD; therefore, it had less available fuel for HTO region which is the main concern of self-sustainability of the ISC.
- To investigate conversion dependence of activation energy, OFW, KAS and Starink models were used. Results of KAS and Starink were close to each other, whereas OFW underestimated E_α values.
- It is better to separately analyze variation of activation energy during LTO, FD and HTO because their reactions schemes are not the same.
- There is no general trend in variation of activation energy over different reaction regions of both heavy and light oils. This is in accordance with the results obtained by Kok et al. [19] and Gundogar et al. [52].
- Isoconversional kinetic modeling showed that activation energy of crude oil may vary considerably with temperature (SD > 20 kJ mL^{-1}); hence, using average E_α value is not recommended. It is better to use isoconversional kinetics in ISC studies. Otherwise, subsequent calculations (e.g., estimation of reaction model) may suffer from significant error caused by assumption of invariant E_α.

References

1. Thomas S. Enhanced oil recovery-an overview. Oil Gas Sci Technol. 2008;63:9–19.
2. Meyer RF, Attanasi ED. Heavy oil and natural bitumen: strategic petroleum resources. U.S. geological survey. FactSheet 70–30, August 2003. http://pubs.usgs.gov/fs/fs070-03/fs070-03.html. Accessed 1 Dec 2010.
3. Tadema HJ, editor. Mechanism of oil production by underground combustion. In: Proceedings of the 5th world petroleum congress, section II, paper 22; 1959.
4. Vossoughi S, Bartlett GW, Willhite GP, editors. Development of a kinetic model for in-situ combustion and prediction of the process variables using TGA/DSC techniques. In: SPE annual technical conference and exhibition; 1982: Society of Petroleum Engineers.

5. Millington A, Price D, Hughes R. The use of thermal analysis techniques to obtain information relevant to the in-situ combustion process for enhanced oil recovery. J Therm Anal. 1993;40(1):225–38. doi:10.1007/BF02546573.

6. Altun NE, Hicyilmaz C, Kök MV. Effect of particle size and heating rate on the pyrolysis of Silopi asphaltite. J Anal Appl Pyrol. 2003;67(2):369–79. doi:10.1016/S0165-2370(02)00075-X.

7. Li J. New insights into the oxidation behaviours of crude oils [Ph.D.]. Ann Arbor: University of Calgary (Canada); 2007.

8. Kok M, Topa E. Thermal characterization and model-free kinetics of biodiesel sample. J Thermal Anal Calorim. 2015;. doi:10.1007/s10973-015-4814-7.

9. Drici O, Vossoughi S. Study of the surface area effect on crude oil combustion by thermal analysis techniques. J Pet Technol. 1985;. doi:10.2118/13389-PA.

10. Kok MV, Hughes R, Price D. High pressure TGA analysis of crude oils. Thermochim Acta. 1996;287:91–9.

11. Kok MV, Acar C. Kinetics of crude oil combustion. J Therm Anal Calorim. 2006;83:445–9.

12. Kok M, Gundogar A. Effect of different clay concentrations on crude oil combustion kinetics by thermogravimetry. J Therm Anal Calorim. 2009;99(3):779–83. doi:10.1007/s10973-009-0377-9.

13. Kok MV. Characterization of medium and heavy crude oils using thermal analysis techniques. Fuel Process Technol. 2011;92(5):1026–31. doi:10.1016/j.fuproc.2010.12.027.

14. Kök MV, Gul KG. Combustion characteristics and kinetic analysis of Turkish crude oils and their SARA fractions by DSC. J Therm Anal Calorim. 2013;114(1):269–75. doi:10.1007/s10973-013-3256-3.

15. Li J, Mehta SA, Moore RG, Ursenbach MG, Zalewski E, Ferguson H, et al. Oxidation and ignition behaviour of saturated hydrocarbon samples with crude oils using TG/DTG and DTA thermal analysis techniques. 2004;. doi:10.2118/04-07-04.

16. Nagabhooshana AA. Studies on pyrolysis and combustion behavior of Neilburg oil and derived asphaltenes using a thermogravimetric analyser (TGA) [M.A.Sc.]. Ann Arbor: The University of Regina (Canada); 2005.

17. Ambalae A, Mahinpey N, Freitag N. Thermogravimetric studies on pyrolysis and combustion behavior of a heavy oil and its asphaltenes. Energy Fuels. 2006;20(2):560–5. doi:10.1021/ef0502812.

18. Ranjbar M, Pusch G. Pyrolysis and combustion kinetics of crude oils, asphaltenes and resins in relation to thermal recovery processes. J Anal Appl Pyrol. 1991;20:185–96. doi:10.1016/0165-2370(91)80072-G.

19. Kok MV, Gul KG. Thermal characteristics and kinetics of crude oils and SARA fractions. Thermochim Acta. 2013;569:66–70. doi:10.1016/j.tca.2013.07.014.

20. Freitag NP, Verkoczy B. Low temperature oxidation of oil in terms of SARA fractions: why simple reaction models do not work. J Can Pet Technol. 2005;44:54–61. doi:10.2118/05-03-05.

21. Benham AL, Poettmann FH. The thermal recovery process—An analysis of laboratory combustion data. Trans AIME. 1958;10:83–5.

22. Burger JG, Sahuquet BC. Chemical aspects of in situ combustion—heat of combustion and kinetics. Soc Pet Eng. 1972;12:410–22.

23. Burger J, Sourieau P, Combarnous M. Thermal methods of oil recovery. Editions OPHRYS; 1985.

24. Ungerer P, Behar F, Villalba M, Heum OR, Audibert A. Kinetic modelling of oil cracking. Org Geochem. 1988;13(4–6):857–68. doi:10.1016/0146-6380(88)90238-0.

25. Sánchez S, Rodríguez MA, Ancheyta J. Kinetic model for moderate hydrocracking of heavy oils. Ind Eng Chem Res. 2005;44(25):9409–13. doi:10.1021/ie050202+.

26. Yağmur S, Durusoy T. Oil shale combustion kinetics from single thermogravimetric curve. Energy Sources Part A. 2009;31(14):1227–35.

27. Hamedi Shokrlu Y, Maham Y, Tan X, Babadagli T, Gray M. Enhancement of the efficiency of in situ combustion technique for heavy-oil recovery by application of nickel ions. Fuel. 2013;105:397–407. doi:10.1016/j.fuel.2012.07.018.

28. Rezaei M, Schaffie M, Ranjbar M. Thermocatalytic in situ combustion: influence of nanoparticles on crude oil pyrolysis and oxidation. Fuel. 2013;113:516–21. doi:10.1016/j.fuel.2013.05.062.

29. Khansari Z, Gates ID, Mahinpey N. Low-temperature oxidation of Lloydminster heavy oil: kinetic study and product sequence estimation. Fuel. 2014;115:534–8.

30. Cinar M, Castanier LM, Kovscek AR. Combustion kinetics of heavy oils in porous media. Energy Fuels. 2011;25(10):4438–51. doi:10.1021/ef200680t.

31. Glatz G. In-situ combustion kinetics of a central european crude for thermal EOR. 2011/1/1/. SPE: Society of Petroleum Engineers; 2011.

32. Fan C, Zan C, Zhang Q, Ma D, Chu Y, Jiang H, et al. The oxidation of heavy oil: thermogravimetric analysis and non-isothermal kinetics using the distributed activation energy model. Fuel Process Technol. 2014;119:146–50. doi:10.1016/j.fuproc.2013.10.020.

33. Bai F, Sun Y, Liu Y, Li Q, Guo M. Thermal and kinetic characteristics of pyrolysis and combustion of three oil shales. Energy Convers Manag. 2015;97:374–81. doi:10.1016/j.enconman.2015.03.007.

34. Varfolomeev M, Nagrimanov R, Galukhin A, Vakhin A, Solomonov B, Nurgaliev D, et al. Contribution of thermal analysis and kinetics of Siberian and Tatarstan regions crude oils for in situ combustion process. J Thermal Anal Calorim. 2015;. doi:10.1007/s10973-015-4892-6.

35. Vyazovkin S. Isoconversional kinetics of thermally stimulated processes. Isoconversional kinetics of thermally stimulated processes. New York: Springer International Publishing; 2015.

36. Ozbas KE, Hicyilmaz C, Kök MV, Bilgen S. Effect of cleaning process on combustion characteristics of lignite. Fuel Process Technol. 2000;64(1–3):211–20. doi:10.1016/S0378-3820(00)00064-3.

37. Richardson MJ, Charsley EL. Chapter 13—Calibration and standardisation in DSC. In: Michael EB, editor. Handbook of thermal analysis and calorimetry. Elsevier Science B.V.; 1998. p. 547–75.

38. Vyazovkin S, Chrissafis K, Di Lorenzo ML, Koga N, Pijolat M, Roduit B, et al. ICTAC Kinetics Committee recommendations for collecting experimental thermal analysis data for kinetic computations. Thermochim Acta. 2014;590:1–23. doi:10.1016/j.tca.2014.05.036.

39. Kök M, Pokol G, Keskin C, Madarász J, Bagci S. Light crude oil combustion in the presence of limestone matrix. J Therm Anal Calorim. 2004;75(3):781–9. doi:10.1023/B:JTAN.0000027174.56023.fc.

40. Kok MVK. Thermo-oxidative reactions of crude oils. J Therm Anal Calorim. 2011;105:411–4. doi:10.1007/s10973-010-1117-x.

41. Dabbous MK, Fulton PF. Low-temperature-oxidation reaction kinetics and effects on the in-situ combustion process. Soc Pet Eng J. 1974;. doi:10.2118/4143-PA.

42. Khansari Z. Low temperature oxidation of heavy crude oil: experimental study and reaction modeling. Calgary: University of Calgary; 2014.

43. Ozawa T. A new method of analyzing thermogravimetric data. Bull Chem Soc Jpn. 1965;38(11):1881–6.

44. Flynn JH, Wall LA. General treatment of the thermogravimetry of polymers. J Res Nat Bur Stand. 1966;70(6):487–523.

45. Doyle C. Estimating isothermal life from thermogravimetric data. J Appl Polym Sci. 1962;6(24):639–42.

46. Starink MJ. The determination of activation energy from linear heating rate experiments: a comparison of the accuracy of iso-conversion methods. Thermochim Acta. 2003;404(1–2):163–76. doi:10.1016/S0040-6031(03)00144-8.

47. Vyazovkin S, Burnham AK, Criado JM, Pérez-Maqueda LA, Popescu C, Sbirrazzuoli N. ICTAC Kinetics Committee recommendations for performing kinetic computations on thermal analysis data. Thermochim Acta. 2011;520(1):1–19.

48. Pu W, Pang S, Jia H, Yu D, Liu M, Wang C. Using DSC/TG/DTA techniques to reevaluate the effect of clays on crude oil oxidation kinetics. J Petrol Sci Eng. 2015;. doi:10.1016/j.petrol.2015.07.014.

49. Rezaei M, Schaffie M, Ranjbar M. Kinetic study of catalytic in-situ combustion processes in the presence of nanoparticles. Energy Sour Recovery Util Environ Eff. 2014;36(6):605–12.

50. Khansari Z, Gates ID, Mahinpey N. Detailed study of low-temperature oxidation of an Alaska heavy oil. Energy Fuels. 2012;26(3):1592–7.

51. Mahinpey N, Murugan P, Mani T. Comparative kinetics and thermal behavior: the study of crude oils derived from Fosterton and Neilburg fields of Saskatchewan. Energy Fuels. 2010;24:1640–5.

52. Gundogar AS, Kok MV. Thermal characterization, combustion and kinetics of different origin crude oils. Fuel. 2014;123:59–65. doi:10.1016/j.fuel.2014.01.058.